Inversión del tensor momento del terremoto de Adra de 1910

Moment tensor inversion of the 1910 Adra earthquake

Daniel Stich[(1)], Josep Batlló[(2)], Jose Morales[(1)], Ramon Macià[(3,4)] and Savka Dineva[(5)]

[(1)] Instituto Andaluz de Geofísica, Universidad de Granada,
Campus Universitario de Cartuja s/n, 18071 Granada, Spain, daniel@iag.ugr.es
[(2)] Dept. Matemática Aplicada I. Universitat Politècnica de Catalunya
[(3)] Dept. Matemática Aplicada II. Universitat Politècnica de Catalunya
[(4)] Laboratori d'Estudis Geofisics Eduard Fontsere. Institut d'Estudis Catalans
[(5)] Dept. of Earth Sciences. University of Western Ontario

ABSTRACT

We examine and model analogue recordings from 6 early mechanical seismographs for the June 16th 1910 earthquake at Adra, Southern Spain. The regional sparse network data were inverted for the deviatoric seismic moment tensor. The best moment tensor solution corresponds to a M_0=1.50e+25 dyne.cm, M_W 6.1 oblique strike-slip event with 91% double couple component. Correlation with available neo- and seismotectonic data clearly favours the 122º/ 80º/ -137º (strike/ dip/ rake) nodal plane as the active fault plane. The 1910 moment tensor shows very good agreement with solutions for 9 small and moderate events, which occurred in the northeastern Alboran Basin between 1997 and 2000, all having strike-slip to normal faulting style and similar orientation of principal axes.

1. INTRODUCTION

On June 16th 1910, southern Spain was struck by a M_W 6.1 earthquake with offshore epicentre in the Alboran Sea, near the coastal town of Adra. The mainshock occurred at 4:16 UTC (Karnik, 1969) and caused destruction corresponding to macroseismic intensity I_0=VIII MSK in Adra, and I_0=VI in the cities of Almeria, Granada and Malaga about 50 to 100 km from the epicentre (Sanchez Navarro-Neumann, 1911). A body wave magnitude of m_b=6.3 (Karnik, 1969) and a surface wave magnitude of M_S=6.1 (Gutenberg and Richter, 1954) have been assigned to this event. Instrumental epicenters for this event were computed about 5 km from Adra (36.7ºN, 3.1ºW, Karnik, 1969), about 15 km from Adra (36.58ºN, 3.08ºW, Vidal, 1986), as well as far-off westward (36.5ºN, 4ºW, Gutenberg and Richter, 1954), however the latter one is clearly inconsistent with the distribution of macroseismic intensity. A major aftershock of magnitude m_b=5.5 occurred at 16:27 UTC (Karnik, 1969).

At the time of the Adra earthquake, seismic recording stations were typically equipped with 2-component, intermediate-period, horizontal sensors, transferring earth motion continuously onto smoked paper. A number of new seismological observatories were forming an early, but very sparse and heterogeneous European seismic network. The 1910 Adra mainshock was recorded at 5 operating Spanish stations and many foreign observatories, and remains still the largest instrumentally recorded crustal earthquake in Spain. The source parameters of this earthquake are of considerable interest for regional seismotectonics and seismic hazard assessment. Another motivation for this study was to learn what source information can be gathered from these historical recordings nowadays.

2. HISTORICAL DATA

We were able to recover paper seismograms of the Adra 1910 mainshock at 6 instruments in Spain, the Netherlands and Italy, and recordings of the major aftershock at 4 instruments in Spain and the Netherlands. These include the Bosch-Omori seismographs at Toledo Observatory (TOL), central Spain, the Grablovitz seismographs at Ebro Observatory (EBR), north-eastern Spain, and at Porto d'Ischia Observatory (PDI), Italy, the Stiattesi seismograph at the 'Collegio alla Querce' Observatory (FIR), Florence, Italy, and both Wiechert and Bosch-Omori instruments at De Bilt Observatory (DBN), Utrecht, the Netherlands (fig. 1).

Obtaining reliable digitised seismogram sections for recordings at the beginning of the 20th century is not a straightforward procedure. The data restoration has been accomplished following Dineva *et al* (2002) and Batlló *et al* (1997): (a) Seismogram scanning: As grey scale images with a resolution of 600-1200 dpi. (b) Digitising: The records were digitised manually with a program providing digitised ASCII points form the raster images. (c) Correction for record curvature and uneven speed: We used the same formulas as those found in Gravovec and Allegretti (1994) and Samardjieva *et al* (1998). (d) Interpolation: The data have been smoothed using linear interpolation to obtain an equal sampling interval of 0.1 seconds. (e) Correction of instrument characteristics of the mechanical sensors (amplification, free period and damping) to obtain true ground displacement seismograms. For TOL and EBR, the contemporaneous bulletin data on instrument characteristics and polarities were double-checked in situ and tested with original instruments. (f) Alignment of the two components at a common reference time, usually synchronous time marks, or the P-arrival for recordings at TOL with unsynchronised time registration.

We want to perform time domain moment tensor inversion and have to confirm if the available recordings satisfy the high quality requirements for this method. The period band which we will use (20 to 50 s) is below the free period of the sensors (between 6 and 20 s) where sensitivity quickly decreases, and first we have to confirm if the Adra 1910 mainshock recordings contain sufficient long period energy. Further we require accurate knowledge of instrument characteristics (polarities), as well as the absence of disturbances like shifts or varying trends in the original recordings. Considering these quality standards we will use the recordings of the mainshock at TOL, EBR and the Wiechert instrument at DBN, but have to discard FIR, PDI and the DBN Bosch-Omori instrument. Recordings of the major aftershock recordings have low signal to noise ratio in EBR (small amplification) and DBN (long epicentral distance), as well as distortion by shifts and trends at TOL and are not suitable for moment tensor analysis.

3. MOMENT TENSOR INVERSION

We inverted for the best deviatoric moment tensor solution by minimising the least-squares misfit between observed long period displacement seismograms and synthetic predictions The synthetic displacements are obtained from 5 independent moment tensor elements and a set of elementary Green's function (Langston *et al*, 1982). Greens functions were generated with a reflectivity algorithm (Kennett, 1983, Randall, 1994), using lithospheric models that have been shown to be capable modelling long period waveforms for events throughout the Ibero-Maghrebian region previously (Stich *et al*, 2002a). The point source Green's functions were convolved with a 4.5 s wide unit-area trapezoidal source time function according to the results of aftershock deconvolution for the Adra earthquake (Stich *et al*, 2002b). The epicentre location was taken from Vidal (1986, latitude 36.58° north, longitude 3.08° west), and the hypocentre depth was left open as it is poorly constrained and has major influence onto the Green's function characteristics. Greens functions were calculated for 15 equidistant depths from 2 to 30 km and alternated in a grid-search.

Our best moment tensor solution fits 69% of the observed long period waveforms as shown in fig. 2. It indicates oblique strike slip faulting and a seismic moment of M_0=1.50e+25 dyne.cm, M_W = 6.1. The major double couple has nodal planes as 122°/ 80°/ -137° and 23°/ 48°/ -13° (values for strike/ dip/ rake respectively). The non double couple component is small (9%) indicating that the long period wavefield of this event is adequately modelled by a simple faulting source. The formally best solution corresponds to a depth of 16 km, slightly deeper than expected in this area where recent seismicity shows a cut-off at about 12 km depth. However the inverted depth is model sensitive and the applied average velocity model does not match local crustal structure at the epicentre (e.g. Banda *et al*, 1993), thus distorting the depth estimate. In any case the obtained solutions do not change significantly between 12 and 22 km depth, indicating a low depth resolution, but a stable mechanism from inversion.

Waveform matches of the inversion result are good at TOL. Also at EBR the similarity is high. The P waves are matched well and the Rayleigh wave prediction matches the amplitudes. The observed phase mismatch can be attributed to complex crustal structure at the eastern coast of Spain. The transverse component at EBR is matched until we cut at the beginning of Love-wave resonance in the sedimentary environment. For the Italian stations (excluded from inversion) the observed amplitudes of body and surface waves are basically consistent with the radiation pattern, except for the transverse component of FIR which is particularly affected by instrumental failures of the FIR NW-SE sensor. At DBN, the near nodal P waves and the S waves are predicted correctly until we cut the traces short before shifts in the surface wave recordings.

Despite the good waveform matches, the very sparse station coverage for this old event rises the question whether the source

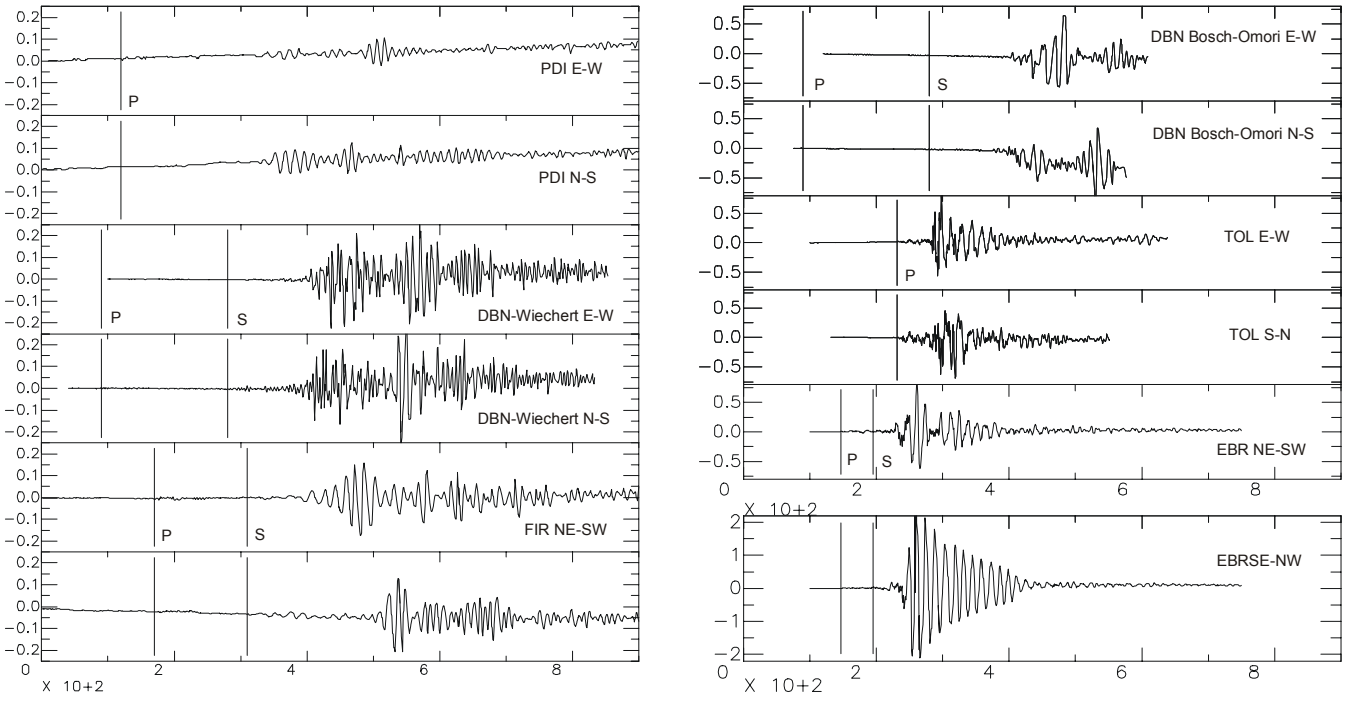

Fig. 1. Historical recordings for the 1910 Adra mainshock from 2-component instruments at TOL, EBR, DBN, FIR and PDI. Traces have been corrected for curvature and amplification, units are in seconds and mm.

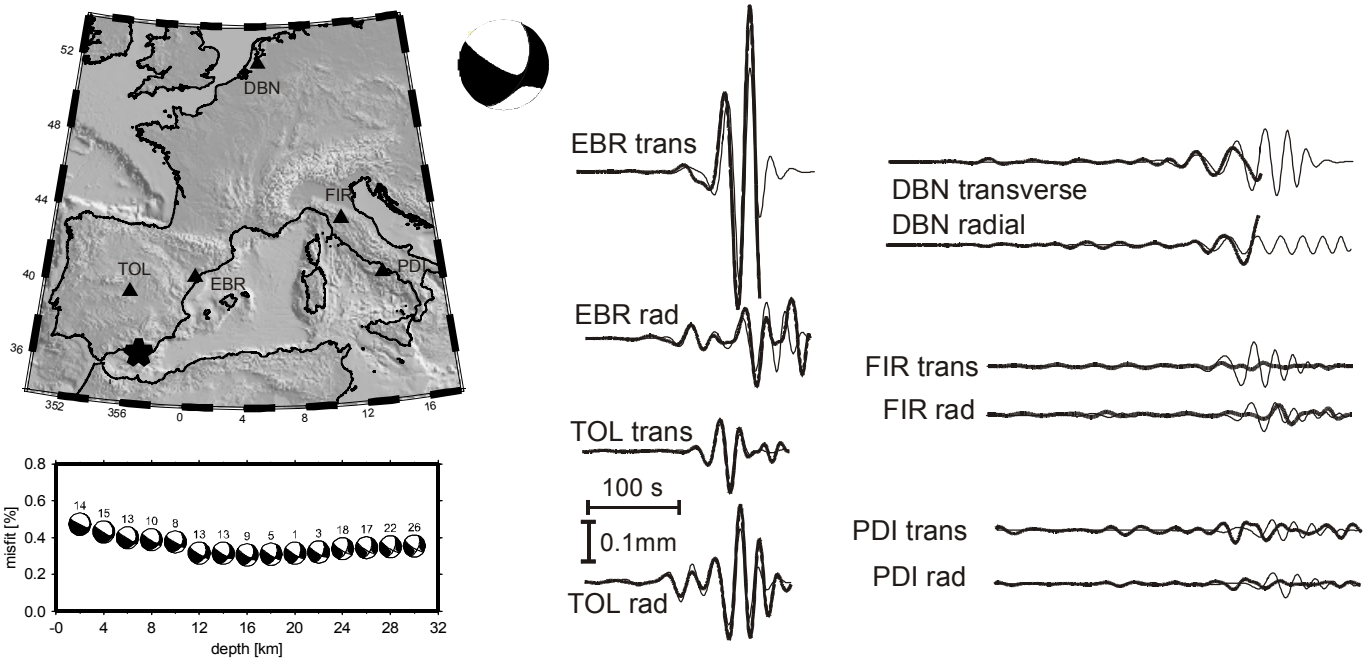

Fig. 2. Best fitting moment tensor solution, corresponding to oblique strike slip faulting at 16 km depth, in lower hemisphere, equal area projection. The inverted mechanisms and misfits for other depths are shown for comparison in the diagram (small numbers next to the mechanisms indicate the percentage of CLVD component for each depth). Waveform matches are illustrated by overlaying observed (thick lines) and predicted (thin lines) long period waveforms, the vertical bar corresponds to 0.1 mm displacement, the horizontal bar to 100 s. All traces start 100 s before the P arrival. Observed seismograms were cut where instrumental failures (DBN) or receiver site resonance phenomena (EBR Love-waves) affected the waveforms.

mechanism is well constrained by the data or if a great variety of source mechanisms are consistent with the available observations. We addressed this question by systematic forward modelling waveforms of alternative double couple mechanisms and analysing their fit to the observed waveforms (Stich *et al*, 2002b). Acceptable alternative solutions were obtained between 12 and 22 km depth. The strike value for both nodal planes and the dip value of the N120°E plane seem to be well resolved (±10°). Larger uncertainties must be assigned to the second dip value and the rake of the N120°E plane (±20°), so we cannot specify the ratio of strike slip and dip slip exactly. The forward modelling procedure clearly rejects solutions with reverse faulting components. In conclusion, the available data constrain the source mechanism surprisingly well, especially the N120°E nodal plane. We attribute this outcome to the fact that one nodal plane intersects between the high quality stations TOL and EBR.

4. TECTONIC INTERPRETATION

The 1910 earthquake occurred near the northern edge of the Alboran Sea basin. Despite its location on the convergent African-Eurasian plate boundary, the Alboran Basin underwent significant crustal extension (e.g. Banda *et al*, 1993), approximately from the early Miocene on (e.g. Docherty and Banda, 1995). Focal mechanism data indicate a nearly east-western orientation of present-day extension (e.g. Mezcua and Rueda, 1997, Stich *et al*, 2002a). The 1910 mainshock was responsible for about 60% of the total moment release in the north-eastern Alboran basin over the last 100 years (ISC on-line Bulletin, http://www.isc.ac.uk/Bull). The moment tensor solution strongly resembles recent regional small to moderate events (fig. 3) with strike-slip to oblique normal faulting style, nearly N-S oriented P-axes (≈N350°E) and nearly E-

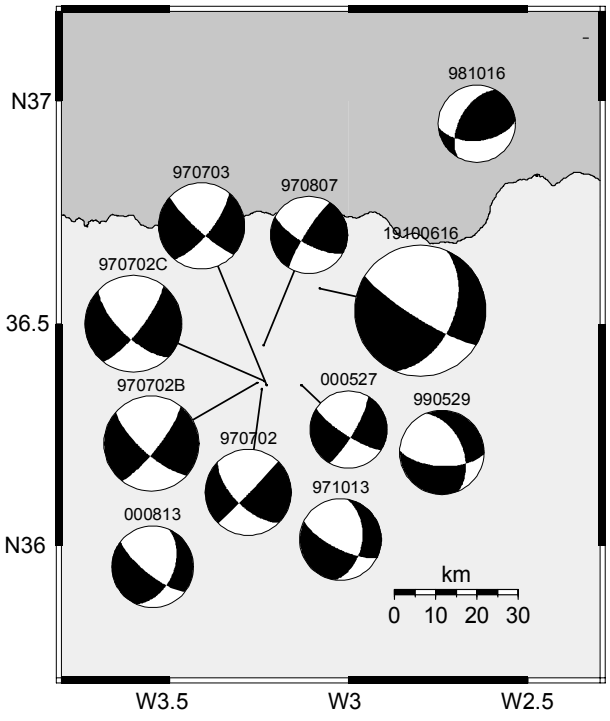

Fig. 3. Comparison of the 1910 Adra earthquake faulting solutions and faulting solutions from regional moment tensors of small tand moderate events (M_w= 3.6 to 4.5) in the northeastern Alboran Basin since 1997.

W oriented T-axes (≈N80°E). This agrees with the neotectonic deformation onshore, characterised by approximately ENE-WSW extension (Rodriguez-Fernandez and Martin-Penela, 1995). We believe that the consistency between historical and recent solutions further supports the inverted moment tensor for the historic 1910 Adra earthquake.

To identify the preferred fault plane among the nodal planes, we considered the pattern of neogene faults in nearby onshore areas. The faults with major recent displacement are steep dipping N120°E to N130°E faults, while other dominant fault directions between N70°E and N90°E show little activity under recent stress conditions (Rodriguez-Fernandez and Martin-Penela, 1995). The orientation of offshore seismogenic structures has been investigated by precise relocations within the seismic series following the moderate M_w 4.8 and 4.9 Adra earthquakes of 1993 and 1994 (fig. 4). Relative locations reveal a clear predominance of N120°E to N130°E oriented active faults and few N60°E to N70°E structures, where the latter ones are possibly reactivated as oversteps for N120-130°E faults (Stich *et al*, 2001). Correlating these neo- and seismotectonic data with the moment tensor solution, we find no neotectonic equivalent for the N23°E plane, but clear evidence for N120-130°E striking, steep dipping faults near the event location. Hence the preferred faulting solution is the right lateral nodal plane with strike 122°, dip 80° and rake of -137°. This implicates a potential to generate destructive earthquakes for the N120º-130ºE faults along the northern edge of the Alboran Basin.

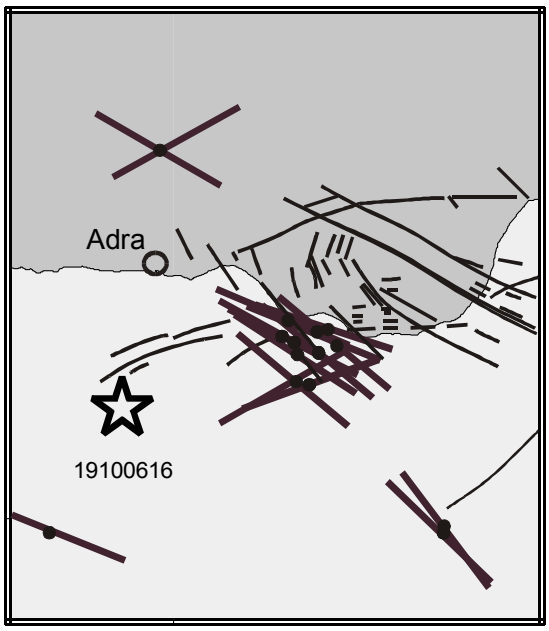

Fig. 4. Evaluation of neo- and seismotectonic data near the site of the 1910 Adra earthquake (star). Strike directions of neogene faults (thin lines, redrawn from Rodriguez-Fernandez and Martin-Penela, 1995) and seismogenic structures (thick lines, obtained from relative locations of multiplet events, Stich et al., 2001) in the epicentral area clearly support that the N122ºE nodal plane was the active fault plane.

5. ACKNOWLEDGEMENTS

We thank the observatories of Toledo, Ebre and De Bilt for providing original seismograms, and G. Ferrari who helped us to obtain the Italian records. We are grateful to Chuck Ammon for discussions on this study. The authors received financial support by the Spanish CICYT, project AMB99-0795-C02-01, by Research Group RNM#104 of Junta de Andalucía and by Spanish DGI projects REN2001-2418, BHA2001-1393 and REN2002-04198-C02-01.

6. REFERENCES

Banda, E., Gallart, J., García-Dueñas, V., Dañobeitia, J.J. and Makris, J., 1993. Lateral variations of the crust in the Iberian Peninsula, New evidence from the Betic Cordillera, *Tectonophysics,* 221, 53-66.

Batlló, J., Susagna, T. and Roca A., 1997. A processing system for old records of regional earthquakes: analysis of the 19 November 1923 earthquake in the Pyrenees, *Cahiers du Centre Européen de Géoynamique et de Séismologie*, 13, 159-175.

Dineva, S., Batlló, J., Mihailov, D. and van Eek, T., 2002. Source paramenters of four strong earthquakes in Bulgaria and Portugal at the beginning of the 20th century, *Journal of Seismology*, 6, 99-123.

Docherty, C. and Banda, E., 1995. Evidence for the eastward migration of the Alboran Sea based on regional subsidence analysis: A case for basin formation by delamination of the subcrustal lithosphere?, *Tectonics*, 14, 804-818.

Grabrovec, D. and Allegretti, I., 1994. On the digitizing of historical seismograms, *Geofizika*, 11, 27-31.

Gutenberg, B. and Richter, C.F., 1954. *Seismicity of the Earth and Associated Phenomena*, Princeton University Press.

Karnik, V., 1969. *Seismicity of the European Area*, Part 1, Reidel, Dordrecht.

Kennett, B.L.N., 1983. *Seismic wave propagation in stratified media*. Cambridge University Press.

Langston, C.A., Barker, J.S. and Pavlin, G.B., 1982. Point-source inversion techniques, *Phys. Earth Planet. Int*., 30, 228-241.

Mezcua, J. and Rueda, J., 1997. Seismological evidence for a delamination process in the lithosphere under the Alboran Sea, *Geophys. J. Int*., 129, 1-8.

Randall, G.E., 1994. Efficient calculation of complete differential seismograms for laterally homogeneous earth models. *Geophys. J. Int*., 118, 245-254.

Rodriguez-Fernandez, J. and Martin-Penela, A.J., 1993. Neogene evolution of the Campo de Dalías and the surrounding offshore areas (Northeastern Alboran Sea), *Geodinamica Acta*, 6, 255-270.

Samardjieva, E., Payo, G. and Lopez, C., 1997. Old regional seismograms at the Toledo observatory. Their study by computer techniques, *Cahiers du Centre Europeen de Geoynamique et de Seismologie*, 13, 159-175.

Sanchez Navarro-Neumann, M., 1911. Los recientes terremotos granadinos (Mayo-Junio de 1911), *Rev. Soc. Astr. de Esp. y Amer.*, 53-56.

Stich, D., Alguacíl, G. and Morales, J., 2001. The relative location of multiplets in the vicinity of the Western Almería (southern Spain) earthquake series of 1993-1994, *Geophys. J. Int*., 146, 801-812.

Stich, D., Ammon, C.J. and Morales, J., 2002. Moment tensor solutions for small and moderate earthquakes in the Ibero-Maghreb region, *J. Geophys. Res*. in press.

Stich, D., Batllo, J., Morales, J., Macia, R. and Dineva, S., 2002. Source parameters of the 1910 M_W=6.1 Adra earthquake (southern Spain), submitted to *Geophys. J. Int*..

Vidal, F., 1986. *Sismotectónica de la región Beticas- Mar de Alborán*, PhD thesis, University of Granada, Granada.